ON THE FORMATION OF CALDERA'S

BY

Dr. B. G. ESCHER.

Published on the occasion of the Fourth Pacific Science Congress
Batavia—Bandoeng (Java).

May 1929.

CONTENTS.

ACKNOWLEDGMENT.

In the following study more mathematics are used than is usual in dealing with problems of dynamical geology. Although the mathematics that are applied are simple, it is only by the help of some colleagues that this study could be carried through. Prof. W. v. d. WOUDE helped me in the solution of the equations of the third degree.

To Prof. Dr. W. de SITTER I owe the elegant method for determining the middle root of the 630 equations of the third degree by a simpler method.

These values were calculated in his institute. To both these colleagues as well as to Prof. EHRENFEST I tender my sincere thanks for the help they gave me.

LEIDEN, Februari 1929.

I. THEORY.

In two previous publications (bibl. 1 and 2) I have brought the formation of calderas into relation with the *gas phase,* observed by PERRET during the eruption of Vesuvius in 1906 (bibl. 3). In these papers I arrived at the conclusion that during the gas phase a cylinder is cored out, and that this may be the cause of caldera formation. In the first paper the subject was treated geometrically, while in the second calculations were made of a particular case (the Krakatoa eruption of 1883) to see if they would bear out this theory. This caldera-formation, however, is not a typical case, as there must previously have been an older Krakatoa-caldera, and in Aug. 1883 it was not a large portion of the volcanic cone that disappeared, but only an island which projected little above sealevel; the northern part of the ancient island Rakata, with the volcanoes Perboewatan and Danan. How a caldera might be formed from a cored-out cylinder I have tried to explain in two different ways. In the case of the Tengger-caldera I assumed, in analogy with what happened in Vesuvius after 1906 (bibl. 3 and 4) that the uppermost part of the cylinder was transformed into a funnel-shape by crumbling away of the walls, and that rising lava, as in Vesuvius 1913—1926, formed a flat bottom which continually reached higher levels.

This explanation does not apply to the caldera of Krakatoa, as after the great eruption of Aug. 26th to 28th 1883 no further signs of eruption were observed, until in Dec. 1927 a new phase began in this famous

volcano. In the case of Krakatoa in 1883, therefore, I thought it justifiable to apply the phenomena, known to occur in coal mining, of recent subsidences which are caused by the working of coal seams lower down.

GOLDREICH (bibl. 5) gives 45° as the angle of inclination of the slides in loose, detrital formations, and a larger angle, as great as 85° for more compact formations (fig. 1).

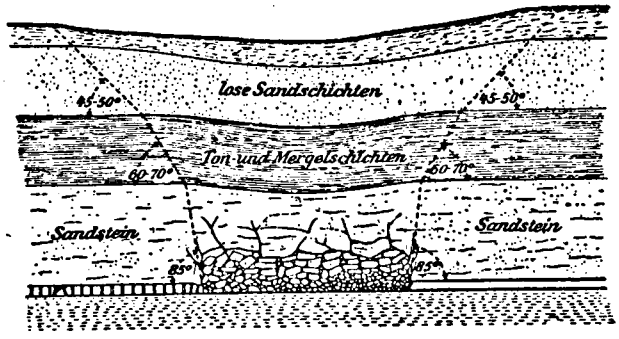

Fig. 1.

Subsidences due to coalmining, according to A. H. GOLDREICH (bibl. 5, p. 88, fig. 59).

If we imagine a sufficiently large disc-shaped mass to be removed from the coal seam, the sliding plane will become funnel-shaped. The applications of this phenomenon to the caldera-formation brought me to the following hypothesis: if not only the cylindrical disc in the depth is removed, but a complete cylinder from the bottom to the surface, à forteriori a funnel-shaped sliding plane [1]) will form, at least if the radius of the eruption cylinder is not too small. The collapsed material will then presumably have a shallow basin-shaped surface. This basin shape might be transformed into a more or less horizontal plane by lava-streams or volcanic ashes or both.

In this article the line of reasoning is resumed, and the last mentioned views on caldera formation from cored-out cylinders are treated as generally as possible. From this, however, it must not be concluded that the first point of view is entirely abandoned, as narrow eruption cylinders will not subside so easily, and the new theory is especially meant for larger eruption cylinders.

If this theory is applied to the normal volcanic cone we arrive at the following results (see fig. 2).

As generating line of the external slope of the volcanic cone a straight line is taken, forming an angle β with the horizontal. The angle of the slide, α, is also measured with regard to a horizontal line. When the cylinder (A A′ B′ B) is expelled from the volcano, the volume

[1]) The term "sliding plane" is used here for the sake of simplicity. It first forms as a funnel shaped fault along which subsequently sliding takes place.

within the surface of revolution (A B C) will collapse into the volume (A A′ D F). The contents of these two bodies must be equal.

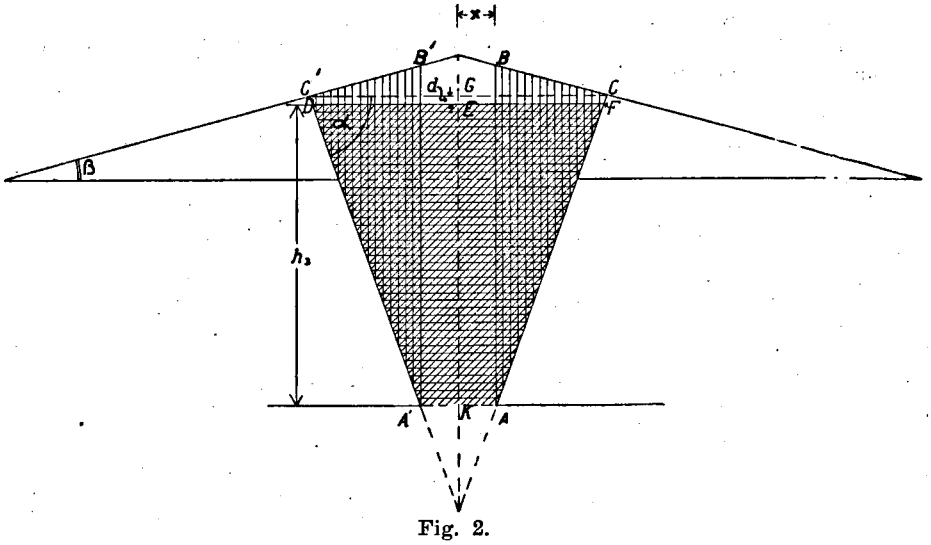

Fig. 2.

Diagram of the formation of a caldera from an eruption cylinder by a funnelshaped slide. R = 1000, d = 50, $\alpha = 70°$, $\beta = 15°$, x = 246, $h_3 = 2021$ (See table B_3).

Of a given caldera R the radius of the upper rim is known as well as *d* the depth below the rim of the caldera bottom, while β and α may vary within certain limits and can be taken as the known variables. The depth $E K = h_3$ of the former eruption cylinder, after the collapse, is a function of α, of the radius of the eruption cylinder x, and in a lesser degree of β also.

In this paper the general equation will be deduced from which x can be found and afterwards h_3. Then a particular case will be treated, and finally a general solution will be given, to which theoretical considerations will be attached.

Of course in reality neither A C not B C will be straight lines and in the calculations, for the sake of simplification, in both cases a mean slope has been taken, while D F has also been taken as straight.

II. CALCULATION.

1. Deduction of the general equation.

Known: R, d, β and α.

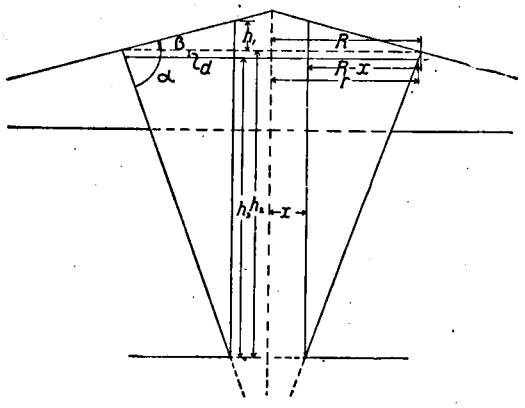

Fig. 3.

The measurements used in the calculation. The drawing was made with: $R = 40$, $d = 3$, $\alpha = 63°26'$, $(\tan\alpha = 2)$, $\beta = 26°34'$ $(\tan\beta = \frac{1}{2})$.

Unknown: x, when:

Contents (A B C) = Contents (A K E F).

$h_1 = (R - x) \tan\beta$

$h_2 = (R - x) \tan\alpha$

$$r = R - \frac{d}{\tan\alpha}$$

$$h_3 = \tan\alpha \left\{ \left(R - \frac{d}{\tan\alpha} \right) - x \right\} \quad \text{(I)}.$$

$$\text{Cont. (A B C)} = \frac{1}{3}\pi (h_1 + h_2)(R^2 + Rx + x^2) - \pi (h_1 + h_2) x^2 =$$

$$= \frac{1}{3}\pi (\tan\beta + \tan\alpha)(R - x)(R^2 + Rx - 2x^2) \quad \text{(II)}.$$

$$\text{Cont. (A K E F)} = \frac{1}{3}\pi h_3 (r^2 + rx + x^2) =$$

$$= \frac{1}{3}\pi \tan\alpha \left\{ \left(R - \frac{d}{\tan\alpha} \right)^3 - x^3 \right\} \quad \text{(III)}.$$

(II) = (III) therefore:

$$\frac{1}{3}\pi(\tan\beta+\tan\alpha)(R-x)(R^2+Rx-2x^2)=$$

$$=\frac{1}{3}\pi\tan\alpha\left\{\left(R-\frac{d}{\tan\alpha}\right)^3-x^3\right\}.$$

$$(2\tan\beta+3\tan\alpha)x^3-3(\tan\beta+\tan\alpha)Rx^2+$$

$$+(\tan\beta+\tan\alpha)R^3-\tan\alpha\left(R-\frac{d}{\tan\alpha}\right)^3=0 \quad \ldots\ldots\ldots \text{(IV)}.$$

2. Example: The Tengger Caldera.

The Sandsea is here taken, whereby the straight boundery, the Tjemora Lawang, is left out of consideration; R = 4000 m., d = 300 m.

What the mean angle of incline β is for the part of the volcanic cone that has disappeared, could only be approximated by a special investigation. The larger the angle is, the larger the volume of the eruption cylinder must be under otherwise equal conditions of the d and R. About 25° would be the maximum that can be assumed for the mean angle of incline. To simplify the calculations $\tan\beta = \frac{1}{2}$ is taken, $\beta = 26°34'$ therefore. For α was taken 45°, 56°19', 63°25', 75°58' and 84°17' successively, sothat $\tan\alpha$ becomes successively: 1, $^3/_2$, 2, 4, 10.

The general equation (IV) then gives the following five equations, together with which the approximated roots are listed, everything being expressed in hectometers.

TABEL A (hectometers).

β	$\tan\beta$	α	$\tan\alpha$	Equation.	Approximate roots.			$h_3(_2)$
					$x(_1)$	$x(_2)$	$x(_3)$	
26°34'	½	45°	1	$8x^3-360x^2+90694=0$	− 13.9	+ 22.4	+ 36.5	14.6
„	„	56°19'	$^3/_2$	$11x^3-480x^2+91384=0$	− 12.2	+ 18	+ 37.8	30.00
„	„	63°26'	2	$14x^3-600x^2+91734=0$	− 11.0	+ 15.5	+ 38.4	46.00
„	„	75°58'	4	$26x^3-1080x^2+92163=0$	− 8.4	+ 10.7	+ 39.2	113.80
„	„	84°17'	10	$62x^3-2520x^2+92585=0$	− 5.7	+ 6.6	+ 39.7	331.00

These five groups of three roots are graphically represented in fig 4. The negative and the smallest positive root approach zero, which is reached at $\alpha = 90°$. The greatest positive root lies close to R, the value of 40 being reached at $\alpha = 90°$.

The negative root has no real significance for our problem, nor has the largest positive root any volcanological importance for our problem,

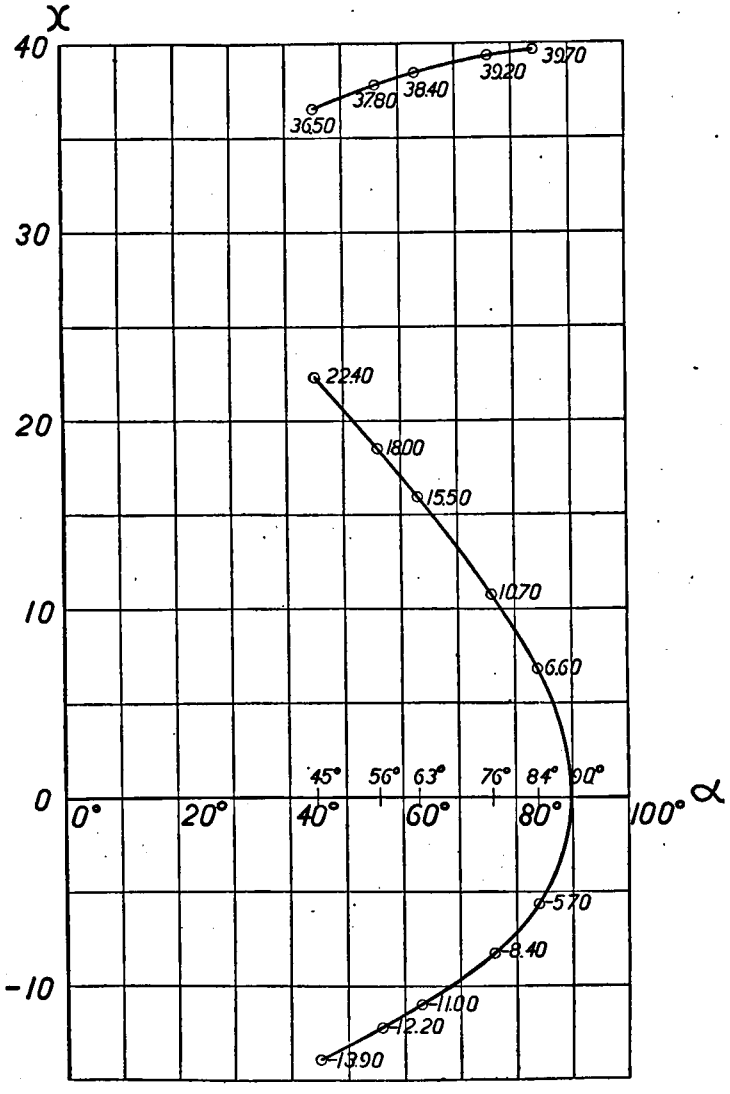

Fig. 4.

Graph of the three roots of the equations of table A.

as the diameter of the eruption cylinder would then be almost equal to that of the caldera and at the same time the depth of the eruption cylinder would be very slight (fig. 5).

It is only the middle root that is of importance, that is the smallest of the two positive roots.

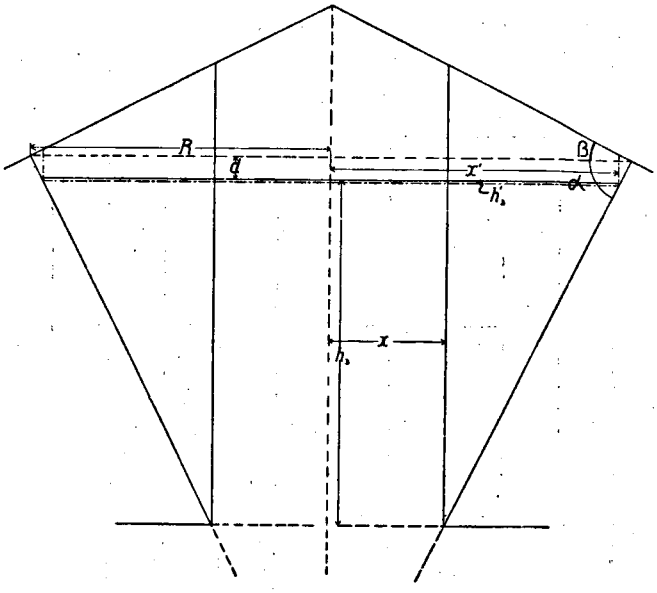

Fig. 5.

Representation of an application of the two positive roots of the equation. $14x^3 - 600x^2 + 91734 = 0$. $R = 40$, $d = 3$, $\alpha = 63°26'(\tan\alpha = 2)$, $\beta = 26°34'(\tan\beta = ½)$. The two positive values of x are 15.5 and 38.4, the values of h_3 belonging to these are 46 and 0.2.

In fig. 6 the equation for the Tengger caldera for $\beta = 26°34'$ and $\alpha = 63°26'$: $y = 14x^3 - 600x^2 + 91734$ is represented graphically. This shows the general course of the functions here dealt with.

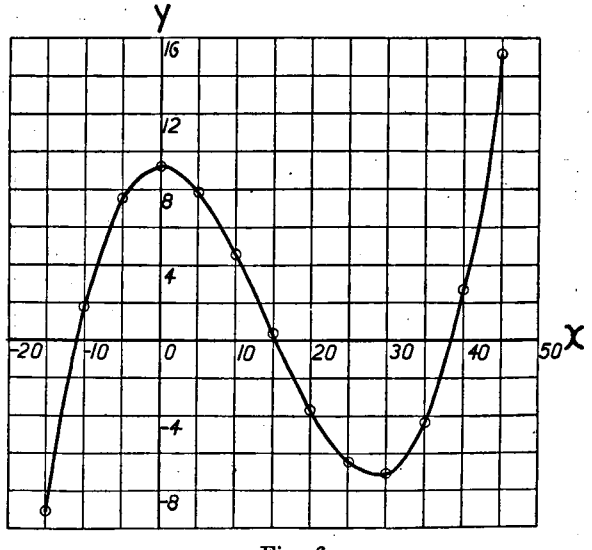

Fig. 6.

Graph of the equation $y = 14x^3 - 600x^2 + 91734$. This equation holds for $R = 40$, $d = 3$, $\alpha = 63°26'$ $(\tan\alpha = 2)$, $\beta = 26°34'$ $(\tan\beta = ½)$. The three roots for x lie on the point of section of the curve with the x-axis $(y = 0)$.

3. General solution.

The solution for the smallest positive root that here follows I owe to Prof. dr. W. DE SITTER, who also had the accompanying 10 tables calculated for me.

As variable knowns besides α and β we have R and d. It is more convenient to take $\delta \left(= \frac{d}{R}\right)$ as known instead of R and d.

By the measurements of a few calderas it was found that δ will usually lie between 0.01 and 0.10.

The following caldera's were consulted:

a. Tengger caldera (Java) (bibl. 1). The "Zandzee", leaving out of consideration the straight boundery of the Tjemoro Lawang.

R = 4000 M., d = 300 M., therefore $\delta = \frac{300}{4000} = 0.075$.

b. Batoer Caldera I (Bali) (bibl. 6 and 7). KEMMERLING (bibl. 6, atlas, plates V and VI) assumes that there must have been an earlier large Batoer caldera, here called I for which I have taken R = 6000 M. and d = 250 M. $\delta = \frac{250}{6000} = 0{,}42$.

c. Batoer caldera II (bibl. 6 and 7). The second Batoer caldera is bounded by the terrace of Kintamani. Following STEHNS map (bibl. 7) for the diameter of this caldera and the same map for the difference in height between caldera rim and caldera bottom, I take R = 3600, d = 300 therefore $\delta = \frac{300}{3600} = 0.083$.

d. Idjen caldera's (Java) (bibl. 8 and 9). KEMMERLING has discovered a terrace on the inner slope of the Goenoeng Kendeng (bibl. 8, p. 57) from which he concludes that in this caldera also, at least two collapses have taken place. Moreover he is of opinion that the elliptic form of this caldera, with a long axis of 20 k.m. from E. to W. and a short axis of 16 k.m. from N to S., indicates a shifting of the volcanic axis. He considers the Idjen to be a composite caldera. For the two Kendeng caldera's KEMMERLING estimates the amount of the two collapses (bibl. 8, p. 140) at 300 m. and 500 m.
Here I have taken for the first caldera formation R = 8000 m., d = 300 and d = 500 m. for the second.

For the first caldera we find $\delta = \frac{300}{8000} = 0.037$.

„ „ second „ „ „ $\delta = \frac{500}{8000} = 0.063$.

If we divide the general equation (IV):

$$(3 \tan \alpha + 2 \tan \beta)\, x^3 - 3 (\tan \alpha + \tan \beta)\, Rx^2 + (\tan \alpha + \tan \beta)\, R^3 - \\ - \tan \alpha \left(R - \frac{d}{\tan \alpha}\right)^3 = 0.$$

by $R^3 \tan \alpha$, it is changed to:

$$\left(3+2\frac{\tan\beta}{\tan\alpha}\right)\left(\frac{x}{R}\right)^3-3\left(1+\frac{\tan\beta}{\tan\alpha}\right)\left(\frac{x}{R}\right)^2+\left(1+\frac{\tan\beta}{\tan\alpha}\right)-\frac{\left(R-\frac{d}{\tan\alpha}\right)^3}{R^3}=0.$$

If we now put:

$$x=\varepsilon R,\ \kappa=\delta\cot\alpha,\ \gamma=\tan\beta\cot\alpha \text{ and } d=\delta R.$$

then the equation:

$$(3+2\gamma)\,\varepsilon^3-3\,(1+\gamma)\,\varepsilon^2+(1+\gamma)-\left\{\frac{(R-R\,\delta\cot\alpha)}{R^3}\right\}^3=0.$$

is arrived at,

$$(3+2\gamma)\,\varepsilon^3-3\,(1+\gamma)\,\varepsilon^2+1+\gamma-(1-\kappa)^3=0\ldots\ldots\quad(V).$$

If we now put:

$$\lambda=1-(1-\kappa)^3=3\kappa\,(1-\tfrac{3}{2}\kappa+\tfrac{1}{3}\kappa^2).$$

We arrive at the equation:

$$\lambda+(1-3\,\varepsilon^2+2\,\varepsilon^3)\,\gamma-3\,(\varepsilon^2-\varepsilon^3)=0\ \ldots\ldots\ldots\quad(VI).$$

This equation is linear in γ and λ for given $\varepsilon\left(=\frac{x}{R}\right)$.

By letting ε vary between $0-0.80$ the equation in λ and γ is expressed in straight lines. From the nomogram thus found with straight lines, on the other hand ε can be read for different γ's and λ's.

By letting α and β increase by 5° different γ's occur, for one particular δ different κ's are then found, and therefore λ's also.

After having found $\varepsilon=\frac{x}{R}$ for 10 different δ's (0.01, 0.02, 0.03..... 0.10), 9 different α's (45°, 50°, 55° ..... 85°) and 7 different β's (0°, 5°, 10° .....·30°), the 630 corresponding values for $\frac{h^3}{R}$ were calculated.

In (I) we found:

$$h_3=\tan\alpha\left\{\left(R-\frac{d}{\tan\alpha}\right)-x\right\}.$$

If we substitute the values found above for $d=\delta R$ and $x=\varepsilon R$ the following equation is arrived at:

$$h_3=\tan\alpha\left(R-\frac{\delta R}{\tan\alpha}-\varepsilon R\right)$$

$$h_3=R\tan\alpha\,(1-\varepsilon)-R\delta$$

therefore:

$$\frac{h_3}{R}=\tan\alpha\,(1-\varepsilon)-\delta\ldots\ldots\ldots\ldots\ldots\quad(VII).$$

The ten tables for the different δ's follow here. (Tables B_1—B_{10}).

If we now wish to apply the reasoning of the new theory to any particular caldera, to see what conclusions we are brought to, R and d must first be ascertained from the topographical map, from which $\delta = \frac{d}{R}$ follows and so shows which of the ten tables must be used.

Corresponding to the tables graphs have been made (fig. 7—16) from which $\frac{x}{R}$ and $\frac{h_3}{R}$ can be read for all α's between 45° and 85° and all β's between 0° and 30°.

Values of β.

From the incline of the remaining foot of a volcano that has been changed into a caldera by collapsing, a mean angle of incline β can be deduced by comparison with the inclination of large volcanic cones that have not been attacked by caldera formation. All β's that belong to a particular angle of α lie upon a straight line in the graphs. For each angle α there is therefore a straight line of β-points; the β-lines for all angles of α bisect eachother at the point $\frac{x}{R} = 1$ and $\frac{h_3}{R} = -\delta$ just above the 0-abscisse therefore, that lies at the top of the graphs. Prof. W. v. D. WOUDE was so kind as to provide me with this important addition.

It enables us to read for one interpolated α-value $\frac{x}{R}$ and $\frac{h_3}{R}$ for the different β-values.

Values of α.

The choice between the different α's seems more difficult. In III this point will be further considered. After a α- and a β-value has been chosen, $\frac{x}{R}$ and $\frac{h_3}{R}$ are read from the graphs or the tables. By multiplying by the particular value for R which we have read from the map, x (= the radius of the cored-out cylinder) and h_3 are found.

TABLE B_1. $\delta = 0.01$.

β \ α		45°	50°	55°	60°	65°	70°	75°	80°	85°
0°	$\frac{x}{R}$	0,103	0,094	0,085	0,078	0,071	0,063	0,055	0,045	0,032
	$\frac{h_s}{R}$	0,887	1,074	1.297	1,587	1,983	2,564	3,51	5.40	11,05
5°	$\frac{x}{R}$	0,214	0,193	0,178	0,160	0,143	0,126	0,111	0,086	0,062
	$\frac{h_s}{R}$	0,776	0,952	1,164	1,445	1,828	2,391	3,31	5,17	10,71
10°	$\frac{x}{R}$	0,282	0,258	0,235	0,216	0,191	0,168	0,144	0,114	0,080
	$\frac{h_s}{R}$	0,708	0,874	1,082	1,348	1,725	2,276	3,18	5,01	10,51
15°	$\frac{x}{R}$	0,348	0,309	0,282	0,258	0,232	0,206	0,174	0,142	0,100
	$\frac{h_s}{R}$	0,642	0,812	1,015	1,275	1,637	2,171	3,07	4,85	10,28
20°	$\frac{x}{R}$	0,385	0,352	0,323	0,294	0,268	0,236	0,202	0,160	0,112
	$\frac{h_s}{R}$	0,605	0,762	0,957	1,213	1,560	2,089	2,97	4,75	10,14
25°	$\frac{x}{R}$	0,427	0,393	0,360	0,328	0,297	0,263	0,228	0,182	0,128
	$\frac{h_s}{R}$	0,563	0,712	0,904	1,154	1,498	2,015	2,87	4,63	9,96
30°	$\frac{x}{R}$	0,466	0,430	0.397	0,362	0,327	0,290	0,250	0,202	0,142
	$\frac{h_s}{R}$	0,524	0,669	0,851	1,095	1,434	1,940	2,79	4,51	9,80

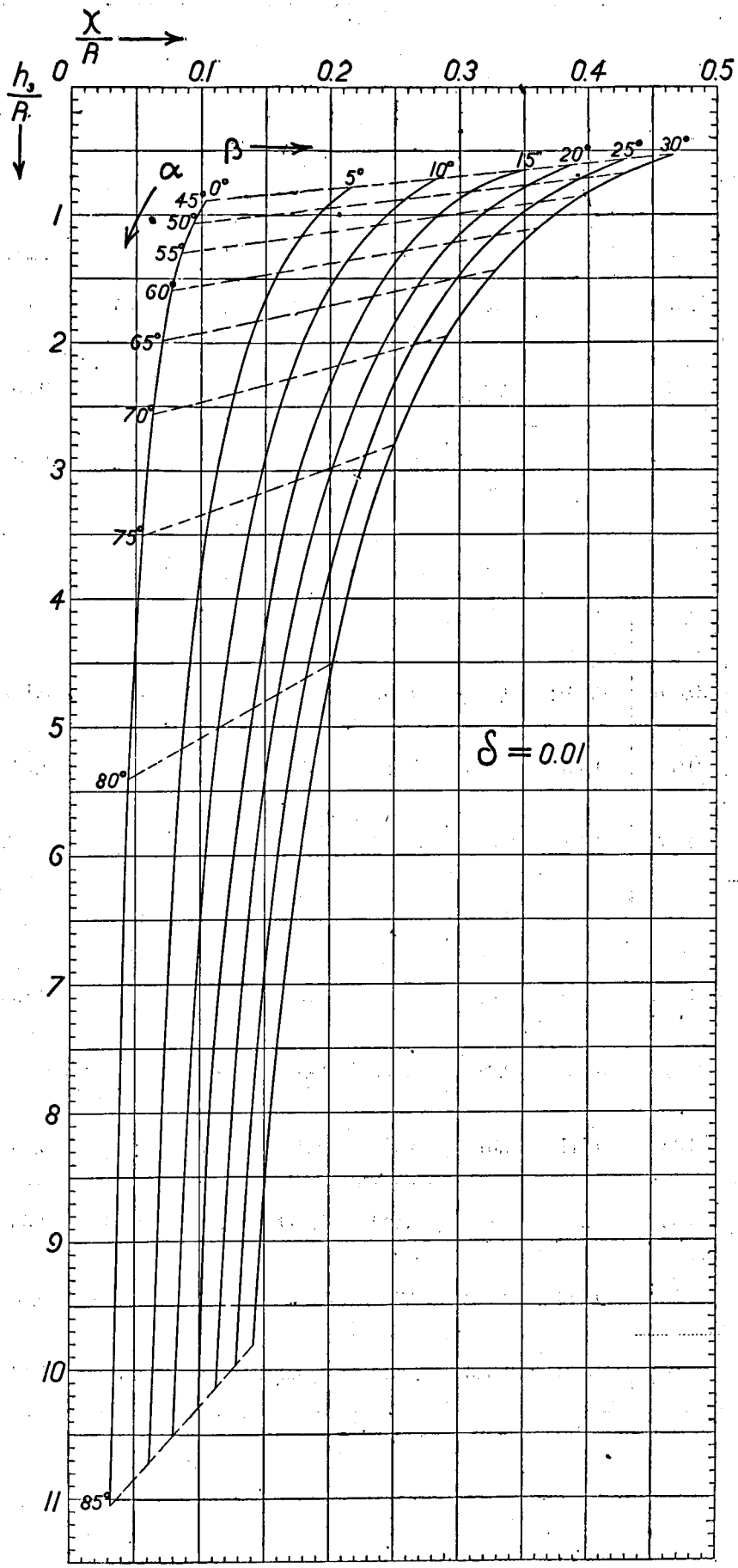

Fig. 7.
Graph of table B_1.

TABLE B_2. $\delta = 0.02$.

β \ α		45°	50°	55°	60°	65°	70°	75°	80°	85°
0°	$\frac{x}{R}$	0,153	0,140	0,126	0,112	0,100	0,087	0,073	0,058	0,046
	$\frac{h_s}{R}$	0,827	1,003	1,228	1,518	1,910	2,488	3,44	5,32	10,88
5°	$\frac{x}{R}$	0,244	0.222	0.201	0,184	0,160	0,141	0,120	0,098	0,070
	$\frac{h_s}{R}$	0,736	0,906	1,121	1,393	1,782	2,340	3,27	5,09	10,61
10°	$\frac{x}{R}$	0,307	0,281	0,254	0,232	0,204	0,180	0,152	0,127	0,086
	$\frac{h_s}{R}$	0,673	0,837	1,045	1,310	1,687	2,233	3,15	4,93	10,42
15°	$\frac{x}{R}$	0,359	0,329	0,300	0,277	0,243	0,213	0,181	0,149	0,103
	$\frac{h_s}{R}$	0,621	0,780	0,980	1,232	1,604	2,142	3,04	4,81	10,23
20°	$\frac{x}{R}$	0,405	0,371	0,339	0,309	0,275	0,244	0,208	0,168	0,116
	$\frac{h_s}{R}$	0,575	0.730	0,924	1,177	1,535	2,057	2,94	4,70	10,08
25°	$\frac{x}{R}$	0,446	0,411	0,374	0,342	0,306	0,271	0,231	0,189	0,131
	$\frac{h_s}{R}$	0,534	0,682	0,874	1,120	1,469	1,983	2,86	4,58	9,91
30°	$\frac{x}{R}$	0,484	0,446	0,410	0,374	0,335	0,297	0,256	0,209	0,146
	$\frac{h_s}{R}$	0,496	0,640	0,823	1,064	1,406	1,911	2,77	4,46	9,74

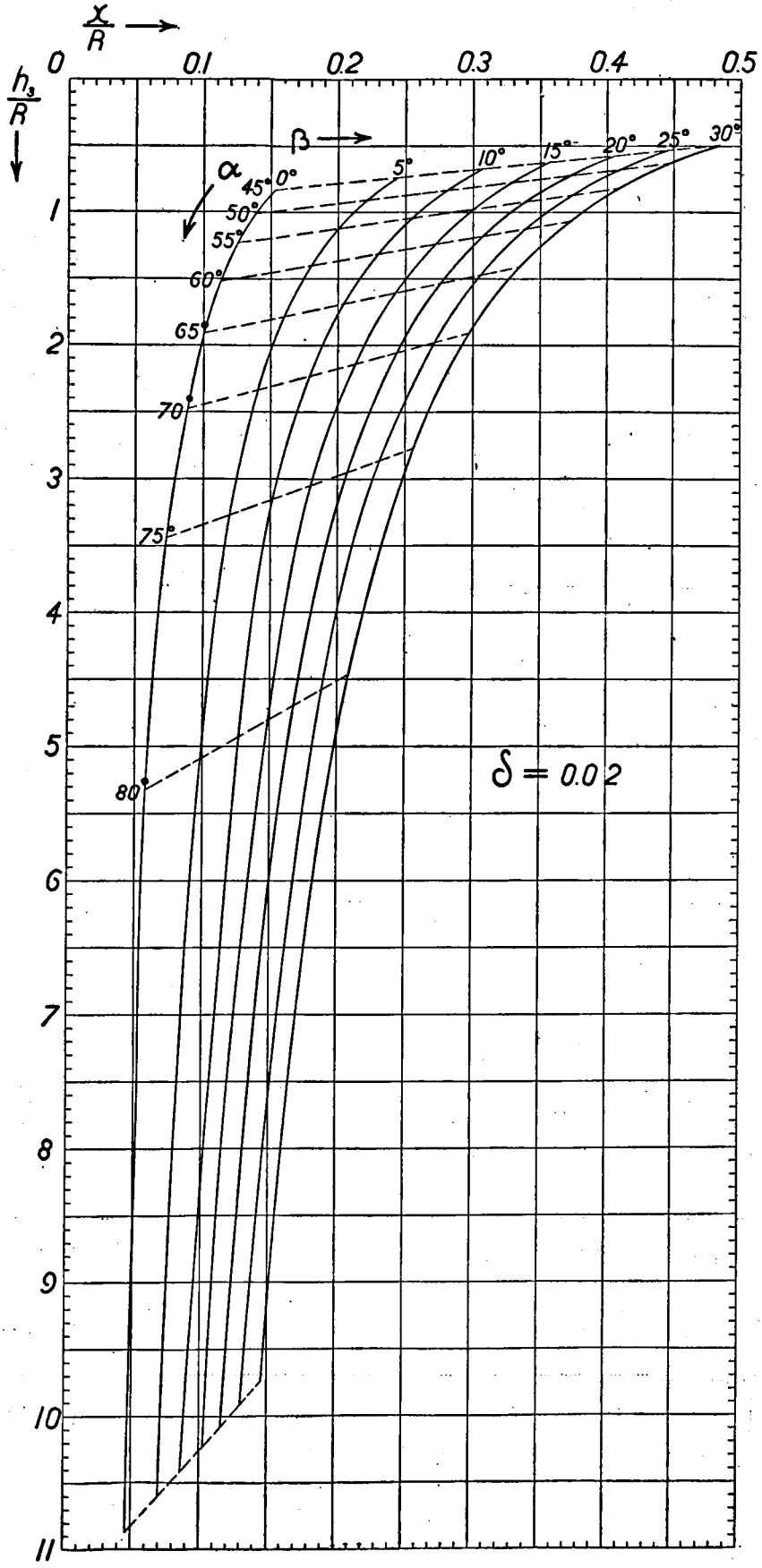

Fig. 8.

Graph of table B_2.

TABLE B_s. $\delta = 0.03$.

$\downarrow\beta$ \ $\rightarrow\alpha$		45°	50°	55°	60°	65°	70°	75°	80°	85°
0°	$\frac{x}{R}$	0,191	0,172	0,158	0,140	0,125	0,110	0,091	0,073	0,057
	$\frac{h_s}{R}$	0,779	0,957	1,172	1,460	1,847	2,415	3,36	5,23	10,75
5°	$\frac{x}{R}$	0,270	0,246	0,225	0,200	0,179	0,158	0,133	0,104	0,078
	$\frac{h_s}{R}$	0,700	0,869	1,077	1,356	1,731	2,283	3,20	5,05	10,51
10°	$\frac{x}{R}$	0,329	0,300	0,272	0,246	0,220	0,194	0,164	0,131	0,093
	$\frac{h_s}{R}$	0,641	0,804	1,010	1,276	1,643	2,184	3,09	4,90	10,34
15°	$\frac{x}{R}$	0,380	0,346	0,316	0,285	0,255	0,227	0,192	0,152	0,109
	$\frac{h_s}{R}$	0,590	0,750	0,947	1,208	1,568	2,093	2,98	4,78	10,16
20°	$\frac{x}{R}$	0,423	0,388	0,356	0,321	0,288	0,254	0,218	0,172	0,121
	$\frac{h_s}{R}$	0,547	0,700	0,890	1,146	1,497	2,019	2,89	4,66	10,02
25°	$\frac{x}{R}$	0,463	0,426	0,390	0,353	0,317	0,282	0,240	0,191	0,136
	$\frac{h_s}{R}$	0,507	0,654	0,841	1,091	1,435	1,942	2,80	4,56	9,85
30°	$\frac{x}{R}$	0,501	0,461	0,422	0,385	0,346	0,306	0,263	0,211	0,150
	$\frac{h_s}{R}$	0,469	0,612	0,795	1,035	1,373	1,876	2,72	4,44	9,69

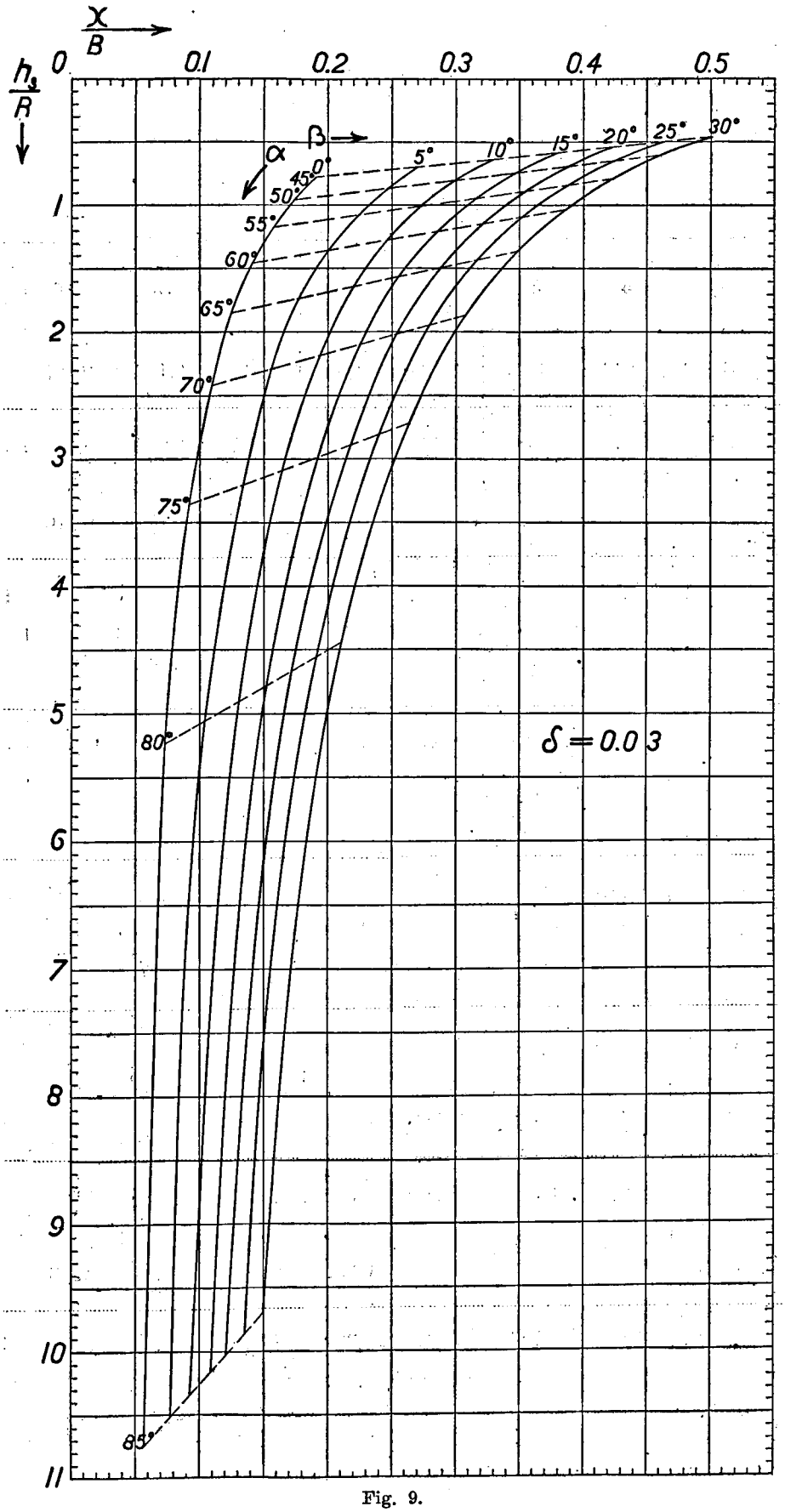

Fig. 9.

Graph of table B_s.

TABLE B_4. $\delta = 0.04$.

$\rightarrow\alpha$ / $\downarrow\beta$		45°	50°	55°	60°	65°	70°	75°	80°	85°
0°	$\frac{x}{R}$	0,224	0,205	0,186	0,166	0,149	0,131	0,112	0,087	0,066
	$\frac{h_3}{R}$	0,736	0,908	1,122	1,404	1,785	2,347	3,27	5,14	10,64
5°	$\frac{x}{R}$	0,294	0,270	0,245	0,220	0,197	0,172	0,148	0,116	0,084
	$\frac{h_3}{R}$	0,666	0,830	1,038	1,311	1,682	2,235	3,14	4,97	10,43
10°	$\frac{x}{R}$	0,352	0,321	0,291	0,262	0,234	0,206	0,176	0,141	0,098
	$\frac{h_3}{R}$	0,608	0,769	0,972	1,238	1,603	2,141	3,03	4,83	10,27
15°	$\frac{x}{R}$	0,401	0,366	0,332	0,299	0,269	0,236	0,202	0,161	0,114
	$\frac{h_3}{R}$	0,559	0,716	0,914	1,174	1,528	2,059	2,94	4,72	10,09
20°	$\frac{x}{R}$	0,442	0,407	0,369	0,333	0,300	0,263	0,227	0,180	0,127
	$\frac{h_3}{R}$	0,518	0,667	0,861	1,115	1,462	1,985	2,84	4,61	9,94
25°	$\frac{x}{R}$	0,482	0,443	0,403	0,366	0,329	0,290	0,248	0,199	0,141
	$\frac{h_3}{R}$	0,478	0,624	0,813	1,058	1,399	1,910	2,76	4,50	9,78
30°	$\frac{x}{R}$	0,518	0,478	0,437	0,397	0,357	0,315	0,271	0,218	0,153
	$\frac{h_3}{R}$	0,442	0,582	0,764	1,004	1,339	1,842	2,68	4,39	9,64

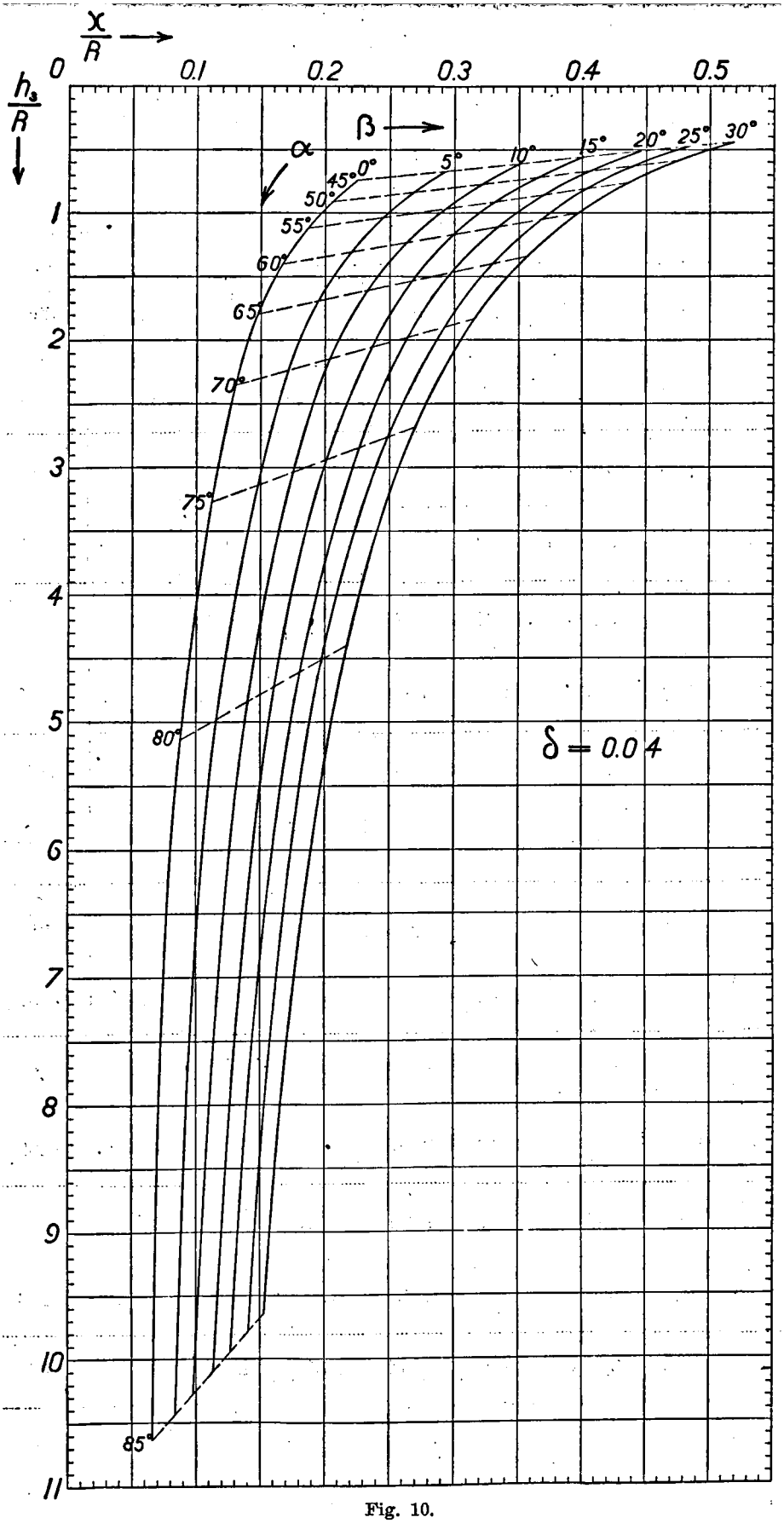

Fig. 10.

Graph of table B_4.

TABLE B_5. $\delta = 0.05$.

β \ α		45°	50°	55°	60°	65°	70°	75°	80°	85°
0°	$\frac{x}{R}$	0,252	0,229	0,208	0,189	0,166	0,146	0,120	0,099	0,065
	$\frac{h_3}{R}$	0,698	0,869	1,081	1,355	1,739	2,296	3,23	5,06	10,64
5°	$\frac{x}{R}$	0,321	0,291	0,262	0,237	0,209	0,183	0,154	0,127	0,085
	$\frac{h_3}{R}$	0,629	0,795	1,004	1,272	1,647	2,194	3,11	4,90	10,41
10°	$\frac{x}{R}$	0,374	0,340	0,307	0,279	0,246	0,216	0,181	0,149	0,098
	$\frac{h_3}{R}$	0,576	0,737	0,940	1,199	1,567	2,101	3,00	4,78	10,26
15°	$\frac{x}{R}$	0,421	0,382	0,348	0,314	0,279	0,246	0,207	0,168	0,112
	$\frac{h_3}{R}$	0,529	0,687	0,881	1,138	1,497	2,021	2,91	4,67	10,10
20°	$\frac{x}{R}$	0,463	0,422	0,383	0,347	0,309	0,272	0,231	0,187	0,127
	$\frac{h_3}{R}$	0,487	0,639	0,831	1,018	1,433	1,950	2,82	4,56	9,93
25°	$\frac{x}{R}$	0,501	0,458	0,418	0,378	0,338	0,298	0,252	0,206	0,140
	$\frac{h_3}{R}$	0,449	0,596	0,781	1,027	1,370	1,878	2,74	4,45	9,78
30°	$\frac{x}{R}$	0,537	0,492	0,450	0,409	0,364	0,322	0,272	0,223	0,154
	$\frac{h_3}{R}$	0,413	0,556	0,735	0,974	1,314	1,812	2,67	4,36	9,62

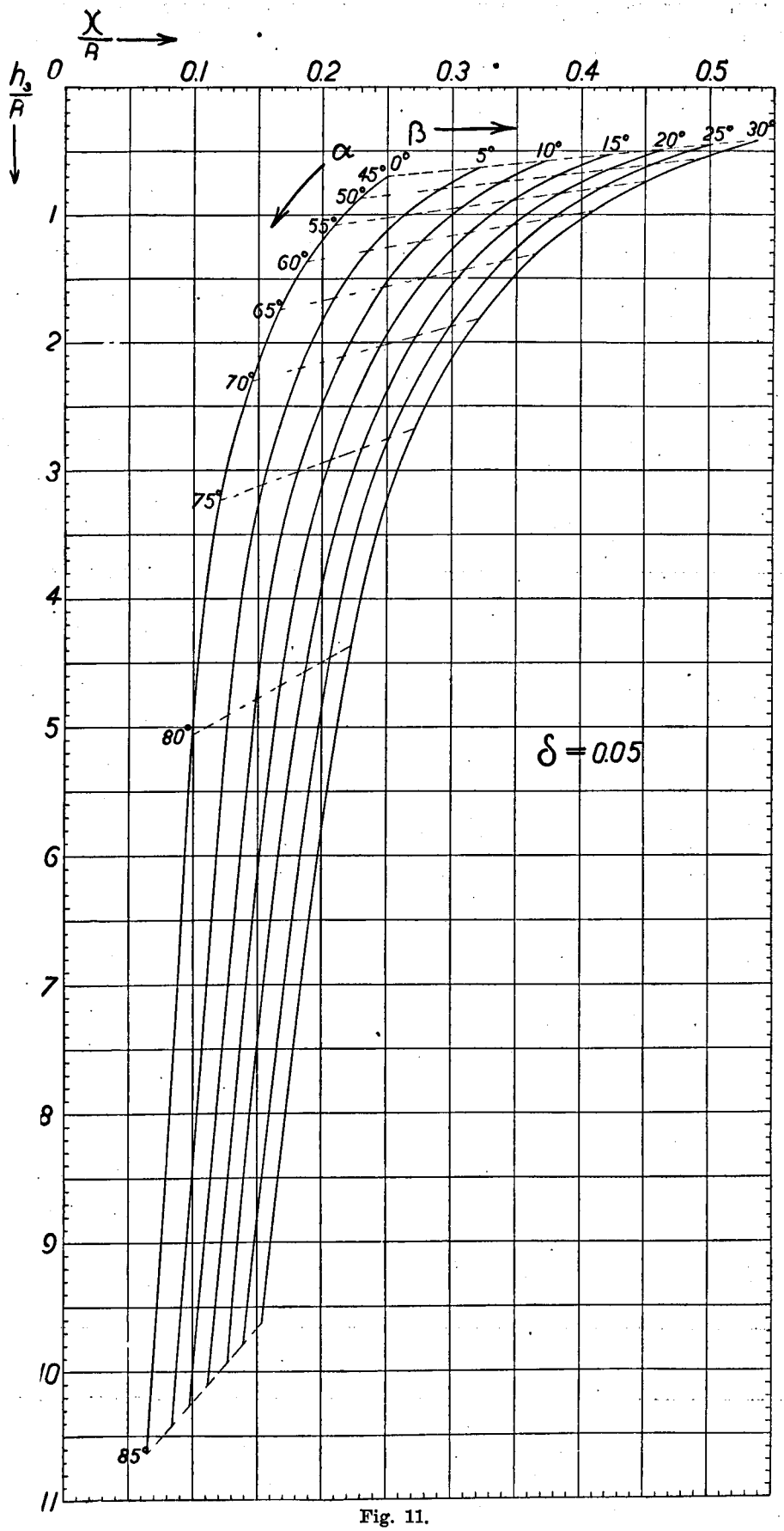

Fig. 11.

Graph of table B_3.

TABLE B_6. $\delta = 0.06$.

β \ α		45°	50°	55°	60°	65°	70°	75°	80°	85°
0°	$\frac{x}{R}$	0,280	0,252	0,229	0,208	0,185	0,162	0,134	0,112	0,073
	$\frac{h_s}{R}$	0,660	0,832	1,041	1,312	1,688	2,242	3,17	4,97	10,54
5°	$\frac{x}{R}$	0,342	0,311	0,282	0,254	0,224	0,198	0,167	0,137	0,091
	$\frac{h_s}{R}$	0,598	0,761	0,965	1,232	1,605	2,143	3,05	4,83	10,33
10°	$\frac{x}{R}$	0,394	0,359	0,324	0,292	0,260	0,229	0,193	0,158	0,104
	$\frac{h_s}{R}$	0,546	0,704	0,905	1,166	1,527	2,058	2,95	4,71	10,18
15°	$\frac{x}{R}$	0,441	0,400	0,364	0,328	0,291	0,257	0,217	0,177	0,120
	$\frac{h_s}{R}$	0,499	0,655	0,848	1,104	1,461	1,891	2,86	4,61	10,00
20°	$\frac{x}{R}$	0,483	0,438	0,399	0,360	0,322	0,282	0,240	0,194	0,132
	$\frac{h_s}{R}$	0,457	0,610	0,798	1,048	1,394	1,912	2,77	4,51	9,86
25°	$\frac{x}{R}$	0,521	0,474	0,432	0,390	0,348	0,307	0,261	0,212	0,145
	$\frac{h_s}{R}$	0,419	0,567	0,751	0,997	1,339	1,844	2,70	4,41	9,71
30°	$\frac{x}{R}$	0,555	0,507	0,463	0,420	0,377	0,332	0,282	0,230	0,158
	$\frac{x}{R}$	0,385	0,528	0,707	0,945	1,276	1,775	2,62	4,31	9,56

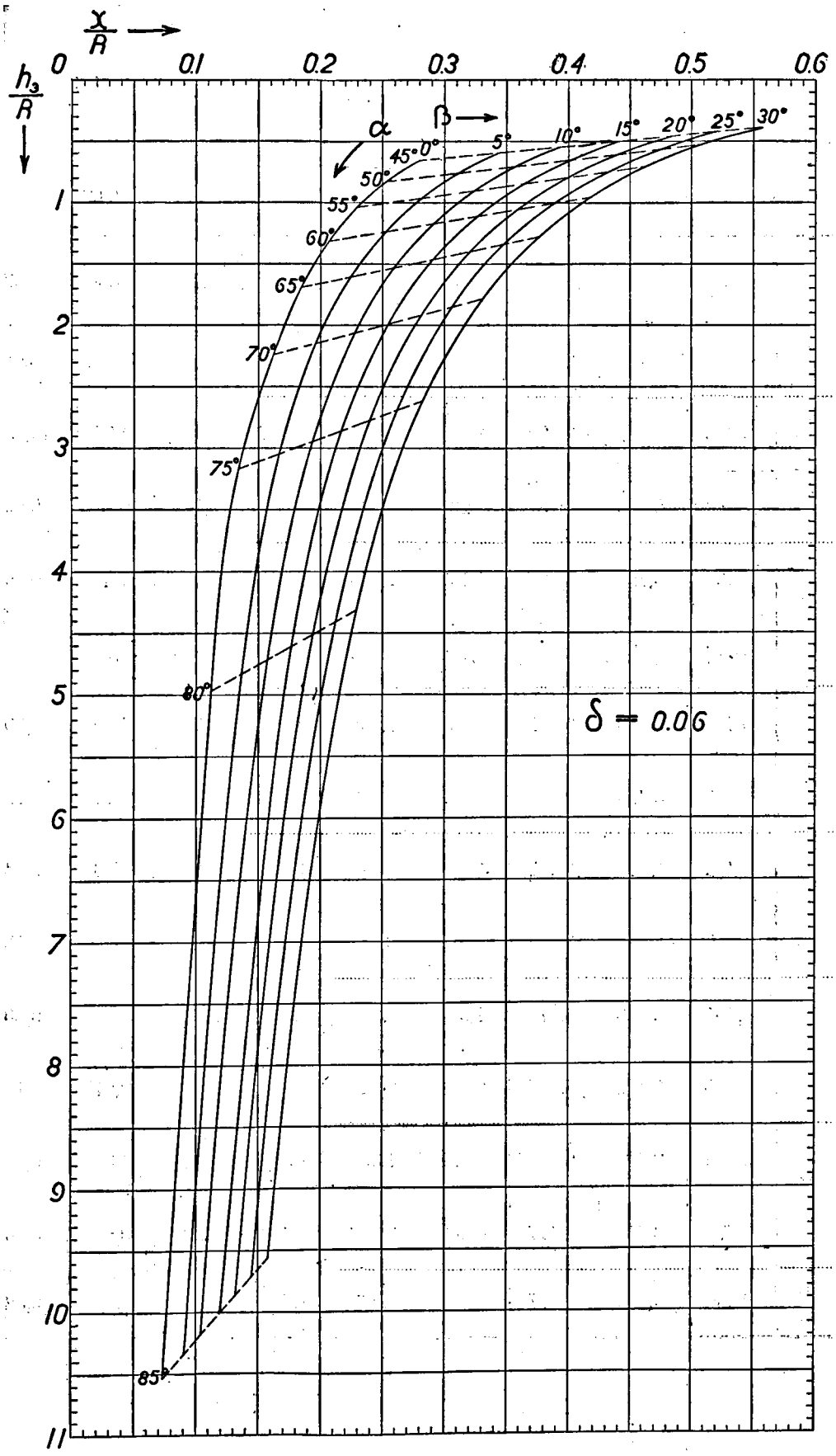

Fig. 12.

Graph of table B_4.

TABLE B_7. $\delta = 0.07$.

β \ α		45°	50°	55°	60°	65°	70°	75°	80°	85°
0°	$\frac{x}{R}$	0,307	0,278	0,249	0,222	0,195	0,172	0,149	0,117	0,080
	$\frac{h_s}{R}$	0,623	0,791	1,002	1,277	1,665	2,205	3,10	4,94	10,45
5°	$\frac{x}{R}$	0,368	0,333	0,298	0,268	0,236	0,207	0,180	0,140	0,097
	$\frac{h_s}{R}$	0,562	0,725	0,932	1,198	1,570	2,108	2,99	4,81	10,25
10°	$\frac{x}{R}$	0,418	0,379	0,341	0,303	0,272	0,238	0,203	0,160	0,110
	$\frac{h_s}{R}$	0,512	0,670	0,871	1,137	1,492	2,023	2,90	4,69	10,10
15°	$\frac{x}{R}$	0,461	0,420	0,379	0,339	0,303	0,263	0,227	0,180	0,124
	$\frac{h_s}{R}$	0,469	0,621	0,817	1,075	1,425	1,955	2,81	4,58	9,94
20°	$\frac{x}{R}$	0,499	0,455	0,412	0,372	0,332	0,289	0,248	0,198	0,137
	$\frac{h_s}{R}$	0,431	0,580	0,770	1,018	1,363	1,883	2,73	4,48	9,80
25°	$\frac{x}{R}$	0,540	0,492	0,445	0,401	0,360	0,314	0,270	0,215	0,148
	$\frac{h_s}{R}$	0,390	0,516	0,723	0,967	1,303	1,814	2,65	4,38	9,67
30°	$\frac{x}{R}$	0,574	0,525	0,477	0,430	0,386	0,338	0,291	0,232	0,161
	$\frac{h_s}{R}$	0,356	0,496	0,677	0,917	1,247	1,749	2,57	4,28	9,52

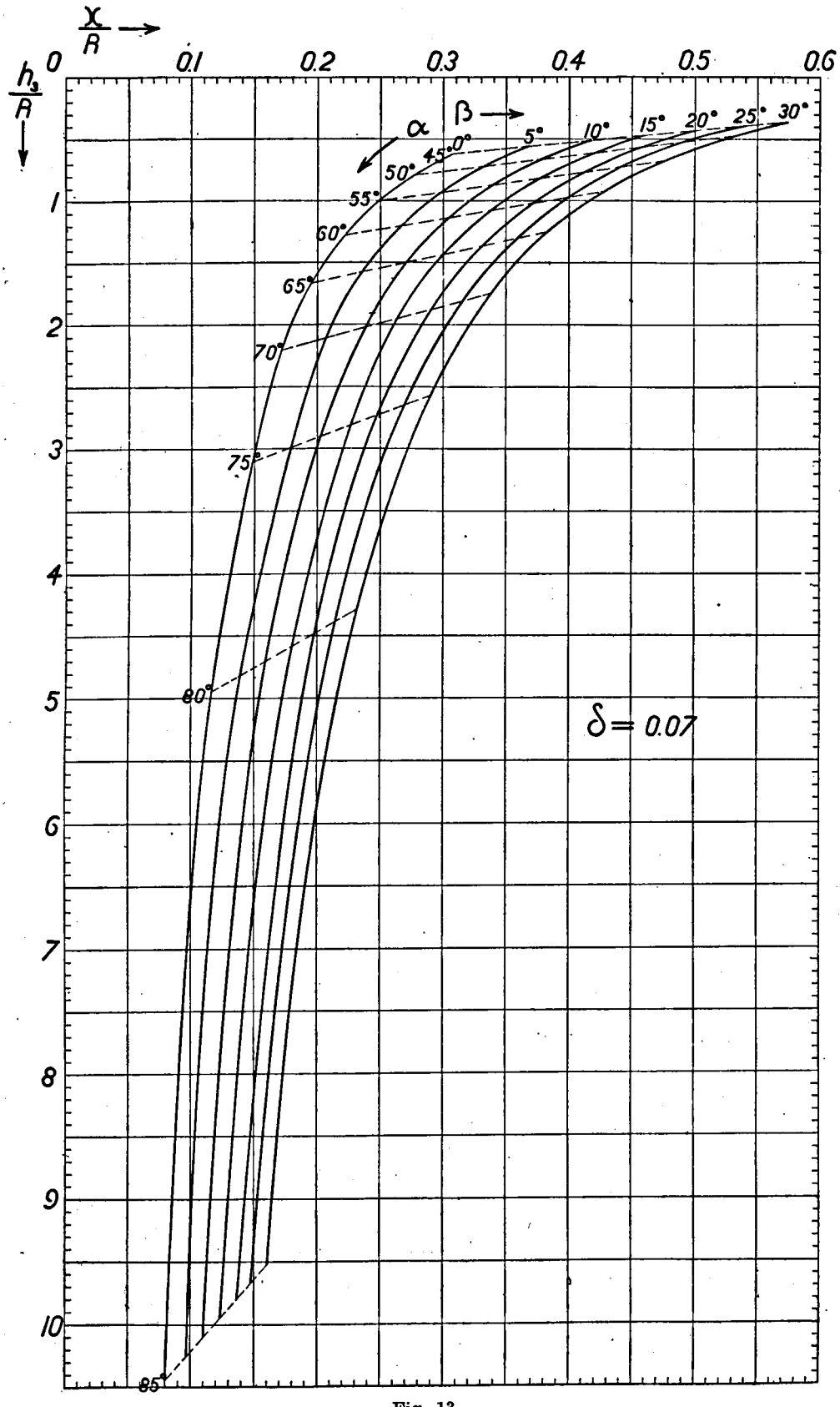

Fig. 13.

Graph of table B_1.

TABLE B_8. $\delta = 0.08$.

β \ α		45°	50°	55°	60°	65°	70°	75°	80°	85°
0°	$\frac{x}{R}$	0,331	0,300	0,271	0,240	0,213	0,188	0,158	0,126	0,087
	$\frac{h_3}{R}$	0,589	0,754	0,961	1,236	1,608	2,151	3,06	4,88	10,36
5°	$\frac{x}{R}$	0,390	0,352	0,318	0,285	0,251	0,220	0,186	0,148	0,103
	$\frac{h_3}{R}$	0,530	0,692	0,894	1,158	1,527	2,063	2,96	4,75	10,17
10°	$\frac{x}{R}$	0,438	0,397	0,357	0,320	0,284	0,249	0,210	0,167	0,116
	$\frac{h_3}{R}$	0,482	0,639	0,838	1,098	1,456	1,983	2,87	4,64	10,02
15°	$\frac{x}{R}$	0,483	0,437	0,393	0,354	0,314	0,276	0,283	0,187	0,130
	$\frac{h_3}{R}$	0,437	0,591	0,787	1,039	1,391	1,909	2,78	4,53	9,86
20°	$\frac{x}{R}$	0,523	0,473	0,427	0,385	0,342	0,299	0,253	0,203	0,141
	$\frac{h_3}{R}$	0,397	0,548	0,738	0,985	1,331	1,846	2,71	4,44	9,74
25°	$\frac{x}{R}$	0,559	0,508	0,459	0,413	0,368	0,325	0,274	0,220	0,152
	$\frac{h_3}{R}$	0,361	0,506	0,693	0,937	1,276	1,774	2,63	4,34	9,62
30°	$\frac{x}{R}$	0,593	0,541	0,492	0,442	0,395	0,348	0,296	0,238	0,165
	$\frac{h_3}{R}$	0,327	0,467	0,645	0,886	1,218	1,711	2,55	4,24	9,46

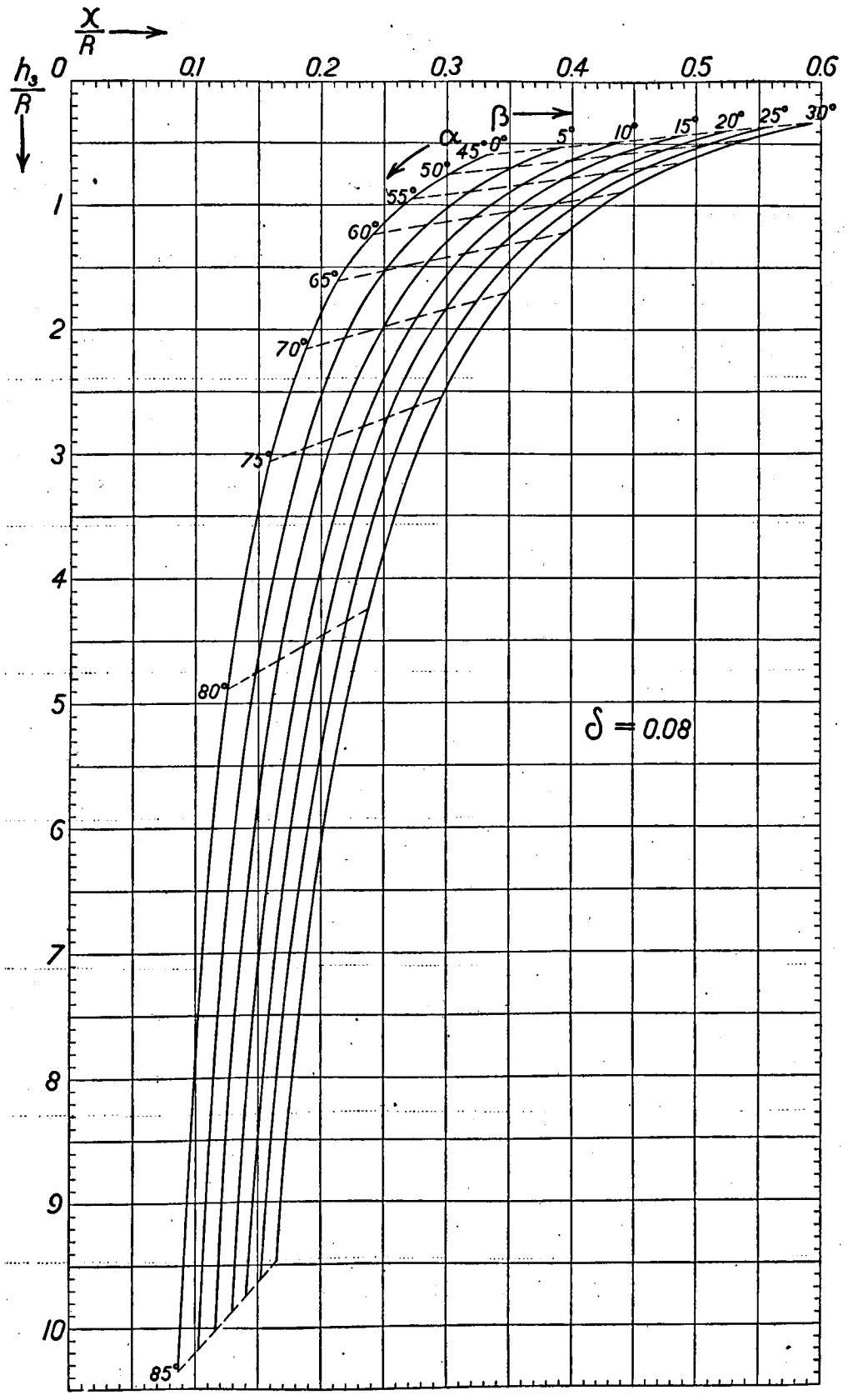

Fig. 14.

Graph of table B_s.

TABLE B_9. $\delta = 0.09$.

β \ α		45°	50°	55°	60°	65°	70°	75°	80°	85°
0°	$\frac{x}{R}$	0,357	0,321	0,288	0,258	0,229	0,200	0,170	0,135	0,093
	$\frac{h_3}{R}$	0,553	0,719	0,927	1,195	1,564	2,108	3,01	4,81	10,28
5°	$\frac{x}{R}$	0,412	0,372	0,333	0,298	0,266	0,232	0,195	0,155	0,108
	$\frac{h_3}{R}$	0,498	0,659	0,862	1,126	1,484	2,020	2,91	4,70	10,11
10°	$\frac{x}{R}$	0,460	0,414	0,372	0,334	0,296	0,260	0,219	0,175	0,120
	$\frac{h_3}{R}$	0,450	0,609	0,807	1,064	1,420	1,943	2,82	4,59	9,97
15°	$\frac{x}{R}$	0,504	0,454	0,408	0,367	0,325	0,285	0,240	0,192	0,135
	$\frac{h_3}{R}$	0,406	0,561	0,755	1,006	1,358	1,874	2,74	4,49	9,86
20°	$\frac{x}{R}$	0,541	0,492	0,441	0,397	0,353	0,309	0,261	0,209	0,145
	$\frac{h_3}{R}$	0,369	0,516	0,708	0,954	1,298	1,808	2,67	4,39	9,68
25°	$\frac{x}{R}$	0,580	0,525	0,472	0,424	0,378	0,332	0,282	0,225	0,156
	$\frac{h_3}{R}$	0,330	0,476	0,664	0,908	1,244	1,745	2,59	4,30	9,56
30°	$\frac{x}{R}$	0,615	0,558	0,503	0,454	0,405	0,356	0,302	0,242	0,168
	$\frac{h_3}{R}$	0,295	0,437	0,620	0,856	1,186	1,679	2,51	4,21	9,42

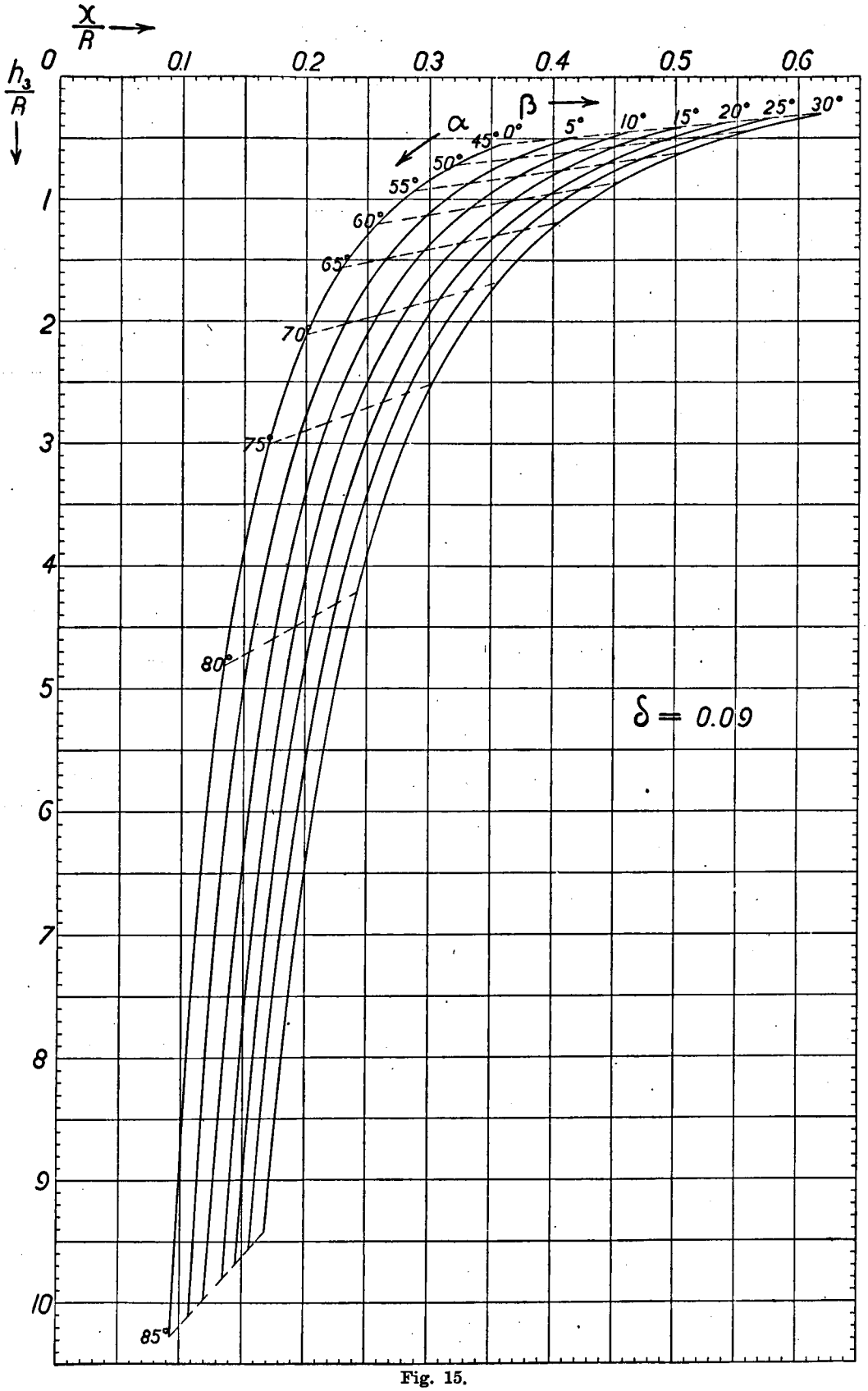

Fig. 15.

Graph of table B_3.

TABLE B_{10}. $\delta = 0.10$.

$\downarrow\beta$ \ $\rightarrow\alpha$		45°	50°	55°	60°	65°	70°	75°	80°	85°
0°	$\frac{x}{R}$	0,382	0,340	0,307	0,272	0,242	0,210	0,181	0,145	0,100
	$\frac{h_3}{R}$	0,518	0,687	0,890	1,161	1,526	2,070	2,95	4,75	10,19
5°	$\frac{x}{R}$	0,437	0,391	0,351	0,313	0,279	0,240	0,206	0,164	0,114
	$\frac{h_3}{R}$	0,463	0,626	0,827	1,090	1,447	1,988	2,86	4,64	10,03
10°	$\frac{x}{R}$	0,485	0,432	0,388	0,347	0,307	0,267	0,228	0,183	0,125
	$\frac{h_3}{R}$	0,415	0,577	0,774	1,031	1,386	1,914	2,78	4,53	9,90
15°	$\frac{x}{R}$	0,527	0,472	0,423	0,380	0,338	0,292	0,250	0,200	0,140
	$\frac{h_3}{R}$	0,373	0,529	0,724	0,974	1,320	1,845	2,70	4,44	9,73
20°	$\frac{x}{R}$	0,567	0,507	0,456	0,409	0,362	0,315	0,270	0,216	0,149
	$\frac{h_3}{R}$	0,333	0,488	0,677	0,924	1,269	1,782	2,62	4,35	9,63
25°	$\frac{x}{R}$	0,604	0,541	0,488	0,438	0,389	0,339	0,289	0,232	0,160
	$\frac{h_3}{R}$	0,296	0,447	0,633	0,873	1,211	1,716	2,55	4,25	9,50
30°	$\frac{x}{R}$	0,640	0,573	0,519	0,465	0,415	0,362	0,309	0,249	0,173
	$\frac{h_3}{R}$	0,260	0,409	0,587	0,827	1,155	1,653	2,48	4,16	9,35

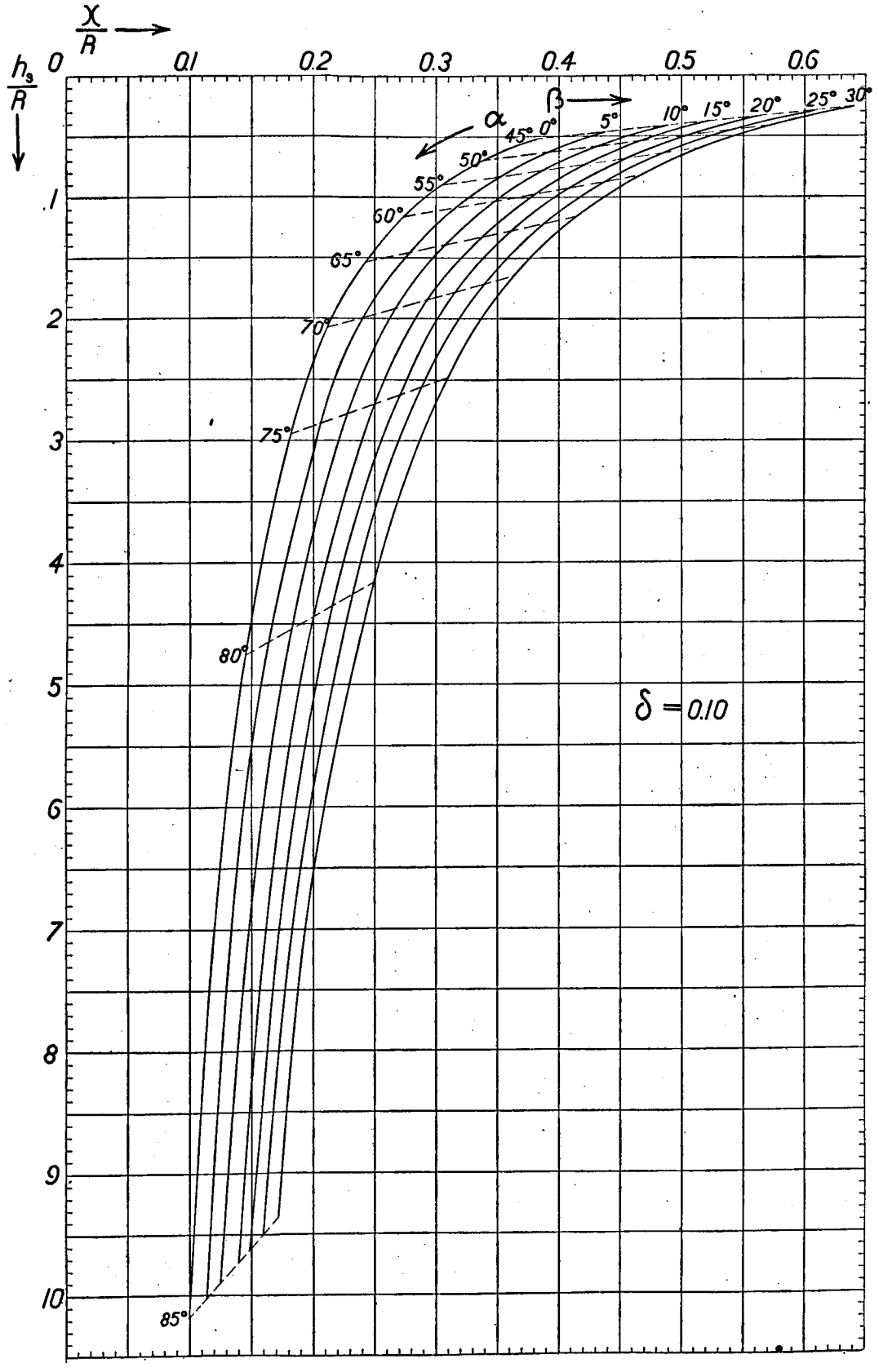

Fig. 16.

Graph of table B_{10}.

III. DISCUSSION OF THE VALUES FOUND, AND THEORETICAL CONSIDERATIONS.

1. On the applicability of the new theory. The values of x.

The theory of the formation of caldera's discussed here is based upon the formation of a cored-out cylinder caused by the gas phase of PERRET (bibl. 3). Secondarily from this cylinder, a caldera is formed by the walls subsiding along a funnel-shaped surface. The formation of a caldera (a negative form), that is to say a large flat crater bottom with steep sides, is a logical consequence of the fact that the angle β is always smaller than the angle α.

The walls of the cored-out cylinder form a vault with a vertical axis which can support radial pressure. It is clear that with uniform material the radius of the cored-out cylinder will decide the amount of pressure that can be supported. The smaller the radius, the greater the pressure that can be born by the vertical arch. It should be possible to make estimations of the relation between these two, but here we will do no more than point out that the radius of the cored-out cylinder of Vesuvius, according to MALLADRA's profile (bibl. 4) is about 100 m., while from FRANK PERRET's work (bibl. 3, p. 67 and fig. 31) the conclusion might be drawn that x lay between 100 m. and 200 m.

After the Vesuvius eruption in 1906 there did not follow any caldera formation, in the manner discussed. The "collapse" of which PERRET (bibl. 3, p. 94) speaks and which he shows in photo's 37 and 56, might be considered as the beginning of a sliding in of the walls. The "external collapse" took place on the south east flank of the cone. It is thought to have been due to a less resistant part of the cored-out cylinder, but I may point out that PERRET explains it in another way. It seems, in fact, that with the Vesuvius-rock the radius $x = 100 - 200$ m. was too small to occasion a caldera formation from collapse. Notwithstanding, the Vesuvius crater gradually acquired a caldera-like shape, caused by the walls of the cylinder crumbling away from above, where the material was loose, and later on by rising lava filling up the vent (bibl. 1, 3 and 4).

Large caldera's, which might also be called *true caldera's* are formed therefore, only when x is large, as it is only then, that the vent can be pressed in. We must not therefore be afraid of assuming a somewhat large radius of the cylinder. This is one of the necessary deductions of the theory developed here: it applies only to spacious cored-out cylinders. If we take the angle $\beta = 15°$, x for $\delta = 0.5$, will be between 0.1 R and 0.4 R that is for $R = 5000$ m. between 500 and 2000 m.

2. On the depth of the cored-out cylinder. The value of h_3.

The depth of the part of the cored-out cylinder that is here called h_3, as also that of the entire original cored-out cylinder, depends primarily

upon the angle α. As soon as α becomes more acute than 70°, h_3 rapidly increases. If we take $\beta = 15°$, h_3 for $\delta = 0.5$ varies between 0.5 R and 10 R. As in comparatively shallow coal mines slides of 85° have been registered in hard rock, it seems to me probable that in our case the mean angle of sliding will be 70° or larger. For $\beta = 15°$ and $\delta = 0.5$, this means that h_3 has a value between 2 R and 10 R. For R = 5000 m., h_3 would lie between 10 km and 50 km. At these depths we approach the magma chamber. For some geologists these depths may seem outrageous, and I must confess that at first sight I found difficulty in accepting such a conclusion, but we shall see that further considerations lead us in the same direction. To make this clear, we must first examine the *degree of force* of a volcanic eruption.

3. On the degree of force of a volcanic eruption.

The motive force of a volcanic eruption is the magmatic gas. As in a violent eruption magma is always thrown out, it cannot be asserted in general that in the magma chamber before the eruption there has been a separation between gas and magma. Before the eruption the gas is in solution under pressure in the magma.

According to the present state of petrological knowledge, I believe, we must suppose that by crystallization of the magma in the depth the gas is held in solution in the residuary magma under a constantly increasing pressure. The increase of pressure can only go as far as the counter-pressure allows. In other words the maximum tension of the gasses dissolved in the residual magma is equal to the resistance of the rock above the chamber.

The pressure of gas at the moment of eruption, that is the initial pressure of the eruption, just exceeds the counter-pressure which is exerted upon the magma chamber. It may be taken that up to depths of 100 km the pressure will increase with a constant ratio to the depth.

Assuming to these depths a mean specific gravity of the rock of 3, the increase of pressure per 10 km will be 3000 kg/cm². At a depth of 50 km the pressure would be 15000 kg/cm². With an eruption from the depth of 50 km the initial pressure would therefore be 15000 kg/cm². There is another factor besides the gas pressure which determines the force of the eruption. This is the length of time during which large quantities of gas per time unite escape. A certain pressure being given by the depth, the force of an eruption will depend upon the total amount of dissolved gas and therefore upon the volume of the magma in the chamber, from which the gas escapes. It is therefore logical to assume, that violent eruptions can only take place, where the magma chamber is large.

The force of a volcanic eruption, therefore, can be physically defined as the product of gas pressure and the amount of gas, and geologically expressed as the function of the depth of the chamber and of its volume.

In 1927 I was able to prove by experiments (bibl. 1), that the radius of a cored-out cylinder is a function of the velocity of the eroding gas.

The velocity itself is a function of the amount per time unite of escaping gas. Further the experiments seemed to show, that at a given pressure a certain amount of time is needed for coring out the cylinder.

The widening begins below and works upwards by eddies to the top, provided there is a sufficient amount of gas available.

Caldera-formation as here described will only take place when the chamber lies deep down, as it is only then that the tension of the gas can be great, and when the volume of the chamber is great, as only then the quantity of gas is sufficient to core out a cylinder. It should be possible to find the depth of the magma chamber from the initial pressure. So far there are no data known on this subject, but is ought to be possible to determine the initial pressure approximately from the gas column of which PERRET gives a representation (bibl. 3, p. 45, fig. 31), as it rose up during the intermediary gas phase in Vesuvius and which only spread out horizontally at a height of 10 km above the vent.

"Let the reader think of globular masses of compressed vapour almost exploding in the air at more than 10 kilometers above the vent, and then try to imagine the original tension of the gas and the degree of its acceleration within the shaft of the volcano" (bibl. 3, p. 45—46).

If it prove feasible to arrive at an idea of the initial pressure in this way and that this is found to be very high, we must not forget that the force of the eruption of Vesuvius in 1906 during the intermediate gas phase was small compared to the force that is needed to form a true caldera via a cored-out cylinder. In the Krakatoa eruption in 1883 the gas column was probably 50 km high, and therefore the minimum depth of the magma chamber much greater than in the Vesuvius eruption in 1906.

4. On the most probable combination of x and h_3.

Returning to what we said on p. 193 and 215 about the angle of α, we must point out in the first place that a given size of the caldera can be arrived at mathematically by various combinations of x with h_3 that differ greatly. For $\delta = 0.5$ and $\beta = 15°$ the combinations vary between $x = 0.4$ R with $h_3 = 0.5$ R with $\alpha = 45°$ and $x = 0.1$ R with $h_3 = 10$ R with $\alpha = 85°$. The point now is to ascertain geologically which combination is the most probable, that with a large h_3 or with a small h_3.

The experiments already described showed that the greater the pressure is in the duct of the gas, the greater the radius of the cored-out shaft becomes. The pressure in the gas duct was measured in a reduction valve. A similar reduction valve will be present in nature, the opening of the magma chamber. But in the natural state the opening will be constantly enlarged by the continuous erosion of the gas-stream. Only when the magma chamber is very large the initial pressure of the escaping gas will be comparatively slowly reduced. Only in that case a spacious cored-out vent can be formed. With a low pressure it is a priori impossible for the vent to be cored-out. It seems to me, therefore, that a combination of great depth and great volume of the magma chamber

are necessary for the formation of a caldera in the way suggested. It follows thus that α must be large.

A steep funnel is the most probable, not only for the reasons given above, but also for the following. The deeper the cause of the sliding down is, the greater must be rigidity of the rock, therefore the greater the angle of slide α must be.

The combination of a large h_3 with a small x seems to me, therefore, the most probable. For a caldera with $R = 5000$ m. and $\delta = 0.5$ and $\beta = 15°$ the most probable combinations would lie between:

$x = 0.1\ R$ with $h_3 = 10\ R$, therefore $x = 500$ m with $h_3 = 50$ km ($\alpha = 85°$).
and $x = 0.2\ R$ with $h_3 = 3\ R$, therefore $x = 1000$ m with $h_3 = 15$ km ($\alpha = 75°$).

5. On the duration of the paroxysms and the periods of quiescence in caldera forming volcanoes.

In bibl. 2 I have endeavoured to show that the cored-out cylinder of Krakatoa in 1883 which led to the caldera being formed, did not lie at the point of the preliminary eruptions which took place from May 20th to Aug. 26th from the Perboewatan volcano amongst others, but about 2 km to the south. R. D. M. VERBEEK had already ascertained (bibl. 10) that the caldera formation of 1883 was not the first, but had been preceeded by a larger one. After the first caldera formation ,according to the theory here developed, the cored-out cylinder must have been choked up by the sliding down material. It is probable that a funnel-shaped vent closed in this way by loose material, will shut off the magma chamber less effectively than the former narrow vent filled with congealed magma. It is also natural that with the increasing gas pressure in the magma chamber the gas will sometimes find an outlet along a weak line in the sliding plane. I regard the formation of the Perboewatan and Danan volcanoes as due to the escape of gas along a sliding plane, just as I regard the present activity of Krakatoa as escape of gas along the sliding plane of 1883. With the leaking out of magmatic gas, magma is carried along and thus a volcano is built up. This stage may continue for a long time. In the case of Krakatoa it probably lasted for centuries. Later on the leakage was choked (1680), so that the pressure in the magma chamber increased more and more during 203 years. On May 20 1883 the weak place was once more opened, the activity gradually increased until on Aug. 26th 1883 the paroxysm took place. The actual eruption from the central vent which formed the cored-out cylinder, began on Aug. 26th 1883, reached its height on Aug. 27th and died out on Aug. 28th at 6 o'cl. in the morning.

The duration of the actual eruption, which caused the caldera formation, was thus very short. This is quite natural, because as soon as a wide channel has been bored by the eroding current of gas, the tension of the gasses dissolved in the magma, quickly decreases. Then the wide eruption channel is choked up and the eruption is over. There was no activity at Krakatoa after Aug. 28th 1883.

It was 44 years, up to Dec. 1927, before the gasses had again acquired sufficient tension to leak out along weak lines in the sliding plane. Presumably, therefore, we are now witnessing the formation of a new series of small secondary Krakatoa volcanoes, again lying excentric with respect to the principle axis. (In other caldera's, such as in Batoer on Bali (bibl. 7) the secondary volcanoes are formed centrally).

To sum up, I think I may conclude, that the paroxysmal eruption which primarily creates a cored-out cylinder and secondarily a caldera, lasts only a very short time, some days, but that the period of rest between two caldera forming eruptions is very long (centuries), that moreover between two paroxysms of the first order a lengthy period of subdued constructive volcanic activity intervenes which may last for centuries. The great depth of the volcanic magma chamber that is here postulated, demands a great length of time to bring about the high gas-pressure necessary to overcome the counter-pressure of the overlying rock. A small leakage has little influence upon the increasing gas-pressure.

Several volcanoes are known in which a caldera formation must have taken place more than once, e. g. Krakatoa, Batoer and Idjen. The rarity with which caldera forming eruptions have taken place in historical time is in itself however a proof that the period of rest between two paroxysms of the first order must be very great.

IV. SYNOPSIS OF THE THEORY OF THE FORMATION OF CALDERAS.

Hypothetical premises.

1. It is possible for PERRET's gas phase to be more violent than in the eruption of Vesuvius in 1906. (PERRET type).
2. The primary result of the gas phase is the formation of a cored-out cylinder and secondarily the collapse of the cylinder along a funnel-shaped sliding plane, formes a caldera.

Conclusions.

1. For this caldera formation a large quantity of gas under high pressure is necessary.
2. A mathematical treatment of the problem leads to the conclusion that the depth of the magma chamber must be great (probably of the order of 15—50 km).
3. Only violent eruptions (paroxysms of the first order) can form a large cored-out cylinder.

   The degree of force of a volcanic eruption is a function of the depth and the volume of the magma chamber.
4. For collapses along sliding planes a wide eruption cylinder is necessary probably of the order of 1000—2000 m).

5. The duration of a paroxysm of the first order (destructive activity) is very short (some days) as compared to the period of quiescence before the next paroxysm of the first order (some centuries).
6. During these centuries the gas pressure must rise to equal the weight of the overlying rocks.
7. During the quiescent period secondary volcanoes may be formed by leakage of gas (constructive activity).

BIBLIOGRAPHY.

1. B. G. ESCHER, Vesuvius, the Tengger Mountains and the Problem of Caldera's. Leidsche Geolog. Mededeelingen, II, pp. 51—88, 1927. (With topographical map of the Tengger-caldera 1: 100.000).
2. B. G. ESCHER, Krakatau in 1883 en in 1928. Tijdschr. Kon. Nederlandsch Aardrijkskundig Gen., 2e Ser., dl. XLV, pp. 715—743.
3. FRANK A. PERRET, The Vesuvius Eruption of 1906. Study of a Volcanic Cycle. Carnegie Institution of Washington, Publication No. 339, Juli 1924.
4. A. MALLADRA, Sul graduale riempimento del cratere del Vesuvio. Communicazione tenuta all' VIII Congresso Geografico Italiano, Vol. II, degl "Atti", 1922.
5. A. H. GOLDREICH, Die Bodenbewegungen im Kohlenrevier und deren Einfluss auf die Tagesoberfläche. Berlin, 1926.
6. G. L. L. KEMMERLING, De Vulkanen Goenoeng Batoer en Goenoeng Agoeng op Bali. Jaarboek v. h. Mijnwezen in Ned. Oost-Indië. 46e Jaarg., 1927, Verhandelingen 1e Gedeelte, Batavia 1918, pp. 50—77. (With Atlas).
7. CH. E. STEHN, De Batoer op Bali en zijn eruptie in 1926. Vulkanologische en Seismologische Mededeelingen, No. 9. Dienst v. d. Mijnbouw in Ned. Indië, Bandoeng 1928. (With map of the Batoer-caldera 1: 50.000).
8. G. L. L. KEMMERLING, Het Idjen-Hoogland, Monografie II. De Geologie en Geomorphologie van den Idjen. Batavia (Without date). (With geological map 1: 100.000 of the Idjen-caldera). Topografische kaart 1: 20.000. Idjen-Hoogland. Toopgrafische Inrichting, Batavia 1920.
10. R. D. M. VERBEEK, Krakatau, Batavia 1885.